JCTC Journal of Chemical Theory and Computation

Article

pubs.acs.org/JCTC

Efficient Computation of Hartree−Fock Exchange Using Recursive Subspace Bisection

François Gygi* and Ivan Duchemin

Department of Computer Science, University of California Davis, Davis, California 95616

ABSTRACT: We use a recursive subspace bisection approach introduced in *Phys. Rev. Lett.* **2009**, *102*, 166406 to accelerate the computation of the Hartree−Fock exchange operator in plane-wave pseudopotential electronic structure calculations. Recursive subspace bisection allows for an unbiased localization of orbitals in domains of varying size and a truncation of orbitals that preserves accuracy in a controlled manner. This representation is used to accelerate the computation of the Hartree−Fock exchange operator, which in turn makes first-principles molecular dynamics simulations based on hybrid density functionals feasible for larger systems than previously possible. We describe a parallel implementation of the method and a load balancing algorithm. The efficiency and accuracy of this approach are demonstrated in electronic structure calculations of a chloride ion solvated in liquid water and calculations of the vacancy formation energy in a 512-atom silicon crystal using the PBE0 hybrid exchange-correlation functional.

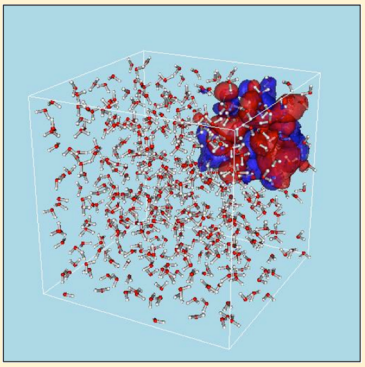

1. INTRODUCTION

Since its introduction in 1965, Density Functional Theory (DFT)[1] has had considerable success in the description of structural and electronic properties of molecules, solids, and liquids.[2] Approximate functionals of increasing complexity were introduced, starting with the Local Density Approximation (LDA)[3] and followed by Generalized Gradient Approximations (GGA) and later orbital-dependent or meta-GGA functionals.[4] In various attempts to improve the accuracy of density functionals, it was noted that the addition of a fraction of the Hartree−Fock (HF) exchange energy to conventional GGA functionals could lead to a better treatment of the exchange interaction, and to a reduction of the self-interaction error that affects most density functionals. The B3LYP functional[5−7] is an example of such a "hybrid" density functional that includes a mixture of gradient-corrected exchange,[5] HF exchange and local correlation[7] in proportions that were adjusted to best reproduce accurate calculated properties for the G2 set of molecules.[8] Other more recent hybrid functionals such as the X3LYP functional[9] or the ωB97 functional[10] were adjusted to reproduce both experimental and accurate theoretical data. Perdew et al. showed that the inclusion of a fixed fraction (1/4) of the HF exchange operator can be justified on theoretical grounds.[11] Adamo and Barone subsequently proposed the PBE0 functional[12] which incorporates this fixed amount of HF exchange. Recently introduced range-separated functionals[13] and long-range corrected functionals[10] were shown to improve considerably the description of electronic properties in a number of systems ranging from molecules to solids.[13,14] In particular, the inclusion of the Hartree−Fock exchange term in the energy functional leads to a large improvement in the calculated HOMO−LUMO gaps of molecules and in the energy band gap of solids. Structural properties are also notably improved.[14] Recently, the use of the PBE0 hybrid density functional in first-principles molecular dynamics simulations has also been shown to improve the description of structural and vibrational properties of liquid water as compared to the PBE GGA functional.[15]

Early implementations of hybrid density functionals were included in quantum chemistry programs using atom-centered basis sets. Implementations based on the plane wave basis were developed later and are still limited to relatively small systems. The plane-wave basis is particularly well adapted for first-principles molecular dynamics simulations due to its translational invariance and absence of basis set superposition errors. These properties have proved critical in order to achieve accurate energy conservation during molecular dynamics simulations.

In this paper, we propose a new approach for the efficient evaluation of the exchange operator, with controlled accuracy. The method relies on the recursive subspace bisection algorithm[16] which allows for an unbiased localization of orbitals in domains of varying size. Using such localized orbitals allows for an efficient computation of the Hartree−Fock exchange operator.

The rest of this paper is organized as follows. In section 2, we discuss the computational cost of Hartree−Fock calculations. Section 3 describes the recursive subspace bisection approach and Section 4, its application to the computation of the Hartree−Fock operator. In section 5, we describe a parallel implementation of the method and a load balancing algorithm. Applications to simulations of a chloride anion in water, the vacancy formation energy in silicon, and the HOMO−LUMO gap in water are presented in section 6.

Received: August 10, 2012

dx.doi.org/10.1021/ct3007088 | *J. Chem. Theory Comput.* XXXX, XXX, XXX−XXX

2. COMPUTATIONAL COST OF HARTREE−FOCK EXCHANGE INTEGRALS

The computation of the Hartree−Fock exchange energy requires the evaluation of exchange integrals involving all pairs of occupied orbitals

$$E_x^{HF} = -\frac{e^2}{2}\sum_{i,j=1}^{N}\int \frac{\phi_i(r)\phi_j(r)\phi_j(r')\phi_i(r')}{|r-r'|}\,dr\,dr' \quad (1)$$

where N is the number of occupied orbitals. If orbitals are expanded on M basis functions, this results in a formal computational cost of $O(N^2M^2)$.

Several methods have been proposed to reduce that cost over the past decades.[17,18] In 1996, Strain et al.,[19] Challacombe and Schwegler,[20] and Burant et al.[21] and later Schwegler et al.[22] and Ochsenfeld et al.[23] developed linear-scaling methods for atom-center Gaussian basis sets. More recently, Yanai et al. proposed a linear-scaling Hartree−Fock approach[24] based on the multiresolution wavelet formulation of Harrison et al.[25]

When using a plane wave basis, the cost of computing the exchange energy scales as $O(N^2M \log M)$ for N electrons and M plane wave basis functions, due to the use of the Fast Fourier Transform (FFT) algorithm in the evaluation of the integrals in eq 1. This cost——if one neglects the log M term——is comparable to that of other parts of a plane-wave electronic structure calculation, which scale as $O(N^2M)$. However, because of the large prefactor associated with the exchange energy computation, this term dominates the computational cost of a plane wave calculation by a large factor and thus severely limits the size of plane wave molecular dynamics simulations including Hartree−Fock exchange. The computation of Hartree−Fock exchange has been implemented in a number of plane wave electronic structure programs including, e.g., Quantum-Espresso,[26] Abinit,[27] and VASP,[28] as well as in methods based on other basis sets such as linear augmented plane waves (LAPW).[29]

Recently, Wu et al.[30] have proposed a method to reduce the cost of the computation of the exchange energy in a plane wave first-principles molecular dynamics simulation. The approach is based on the computation of maximally localized Wannier functions (MLWF)—or Boys orbitals[31]—followed by a truncation of orbitals outside of domains of fixed size. This approach was shown to accelerate the computation of the exchange energy in a simulation of liquid water, in which the spread of Wannier functions can be reliably predicted, and where an appropriate choice of localization region can be made to enclose Wannier functions.

In more complex systems (e.g., for ions solvated in water or at metal−insulator interfaces), Wannier functions can exhibit a wide range of spreads. These spreads are also expected to change during the course of a molecular dynamics simulation depending on bonding configurations. The truncation of orbitals in fixed localization regions in such situations can result in uncontrolled errors in the Hartree−Fock exchange energy.

3. RECURSIVE SUBSPACE BISECTION

The recursive subspace bisection (RSB) approach provides a representation of the subspace of occupied orbitals in terms of localized orbitals.[16] The RSB algorithm consists of defining a set of Walsh projectors $P^{(k)}$ associated with subdomains Ω_k of the unit cell. An approximate simultaneous diagonalization of the Walsh projectors in the subspace of occupied orbitals yields an orthogonal transformation that generates orbitals that are maximally localized in the subdomains Ω_k. When used with multiple levels of recursion, the RSB approach generates a representation of a Slater determinant in terms of orbitals localized on a hierarchy of rectangular domains of varying size, ranging from the full simulation cell down to small domains obtained by repeated bisection of the unit cell. After performing the RSB transformation, the degree of localization of an orbital $\phi_i(r)$ in a subdomain Ω_k is given by the singular value (or cosine) $c_i^{(k)}$ of the Walsh projector $P^{(k)}$ associated with the orbital i. Specifically, the 2-norm of the projection of the orbital $\phi_i(r)$ on the subdomain Ω_k satisfies

$$\int_{\Omega_k} |P^{(k)}\phi_i(r)|^2 dr \geq (c_i^{(k)})^2 \quad (2)$$

This property allows one to truncate orbitals in subdomains while controlling the 2-norm error caused by the truncation procedure. Selective truncation of orbitals is performed as follows. A threshold $\varepsilon > 0$ is first chosen. Each orbital ϕ_i is then truncated to zero outside of the domain Ω_k if the singular value $c_i^{(k)}$ satisfies $(c_i^{(k)})^2 > 1 - \varepsilon$. This guarantees that the error in 2-norm due to the truncation is smaller than $\sqrt{\varepsilon}$. It is important to note that this procedure can truncate different orbitals to subdomains of different shapes and sizes.

The degree to which an orbital can be localized and truncated at a given threshold ε depends on the physical properties of the system. It was shown in ref 16 that in insulators, orbitals can be localized and truncated to small domains with small thresholds, while in more complex systems containing a mixture of insulating and semiconducting subsystems, various degrees of localizations can be obtained. In particular, some orbitals cannot be localized to small domains. The RSB procedure naturally captures this variability in the localization properties of orbitals.

The RSB algorithm provides a systematic way of reducing the amount of information needed to describe electronic orbitals. In a dense system such as, e.g., liquid water, the number of degrees of freedom needed to represent all orbitals in a Slater determinant is NM and is therefore proportional to N^2 since the number of basis functions M grows like N. The use of recursive bisection reduces this number to $O(N \log N)$ while preserving control over the approximation made in truncations.[16]

4. EFFICIENT COMPUTATION OF THE HARTREE−FOCK EXCHANGE OPERATOR

The compact representation of orbitals described in the previous section can be used to reduce the cost of the computation of the Hartree−Fock exchange energy. The large cost of the computation of the exchange energy in the plane wave basis results from the large number of orbital pairs included in the double sum in eq 1. The localization properties of orbitals computed with the RSB approach can be used to truncate the sum by selecting pairs of orbitals that have a sizable 2-norm in a common subdomain. Thus an exchange integral

$$K_{ij} = -\frac{e^2}{\Omega}\int \frac{\phi_i(r)\phi_j(r)\phi_j(r')\phi_i(r')}{|r-r'|}\,dr\,dr' \quad (3)$$

is *not* computed if there is at least one Walsh projector $P^{(k)}$ that "separates" the two orbitals $\phi_i(r)$ and $\phi_j(r)$ for a given value of the threshold, i.e., if $(c_i^{(k)})^2 < \varepsilon$ and $(c_j^{(k)})^2 > (1 - \varepsilon)$. It should

dx.doi.org/10.1021/ct3007088 | J. Chem. Theory Comput. XXXX, XXX, XXX−XXX

be noted that the set of exchange integrals selected in this way may vary between successive self-consistent iterations. We have found that this variation does not introduce instabilities or slow down the convergence of the calculation.

Selecting exchange integrals in this way leads to a large reduction in the computational cost of the exchange energy as will be shown quantitatively below. This criterion provides an objective way of selecting exchange integrals with controlled accuracy. Control of the accuracy resides in the ability to reduce the error by reducing the value of the threshold ε continuously to zero, which in turn restores the full cost of the original computation. In large, insulating systems, we find that the cost of the exchange energy can be reduced from $O(N^3 \log N)$ to approximately $O(N^2 \log N)^2$ using this approach.

In the current implementation of the selective truncation scheme, we evaluate exchange integrals by integration over the entire unit cell. This is not strictly necessary since in most cases the truncated orbitals are nonzero only in a limited common subdomain. Computing exchange integrals on such limited domains could be exploited to further reduce the cost of the computation, potentially leading to a cost of $O(N \log N)$. In the context of a plane wave basis implementation, the integration on limited domains is more complex and will only be considered in a future investigation.

Computing exchange integrals on the entire cell however preserves a useful property of the truncation error. Since each exchange integral K_{ij} is negative (as is easily seen from a Fourier representation of the integral), the error due to the selective truncation scheme is guaranteed to be positive. This provides a way of verifying the convergence of the error in the limit $\varepsilon \to 0$ since the exchange energy approaches the exact value from above. We note that acceleration methods based on the selection of orbital pairs using Schwarz inequalities were discussed by Whitten[17] and Häser and Ahlrichs.[18]

5. PARALLEL IMPLEMENTATION IN THE PLANE WAVE BASIS

Our implementation of the Hartree−Fock exchange operator in the plane wave basis closely follows the procedure described in ref 32. Exchange integrals are computed using Fourier transforms of orbitals and a Fourier representation of the Coulomb interaction. Recursive subspace bisection is first performed, and a localization vector is computed and associated with each orbital, describing the subdomains in which it is localized for a given value of the threshold ε. Localization vectors are then used to select exchange integrals.

In the absence of recursive bisection, the number of exchange integrals is fixed at $(N(N+1)/2)$, and the computation can be easily distributed over concurrent processes in a parallel computer. The approach described in ref 32 provides an efficient and scalable way to compute the exchange energy in that case. If however exchange integrals are selected on the basis of their localization properties, load balancing issues may arise, which could negatively affect the efficiency of the exchange energy calculation. We adopt a load balancing strategy that redistributes orbitals among groups of processors according to their localization domains. This procedure is best described using a representation of the computational task in terms of a graph. This *task graph* includes N vertices, each of which represents an orbital. Exchange integrals are associated with edges of the task graph. In a conventional Hartree−Fock calculation in which all exchange integrals are computed, the task graph is a complete N graph; i.e., the number of edges is $N(N+1)/2$. The selective truncation procedure removes edges from the task graph according to the value of the threshold ε. The properties of the resulting (sparse) graph can be used to divide the computational task evenly among processors. Since the cost of computing an exchange integral K_{ij} is the same for all pairs (i,j), an equal weight can be associated to all edges of the graph. When expressed in this way, the load balancing procedure is equivalent to partitioning the task graph into equally weighted subgraphs. Ideally, orbitals should be distributed among processors in such a way that an equal amount of work must be performed on each processor. An ideal distribution of the work amounts to defining a sequence of optimal partitions of the task graph that defines how orbitals are initially distributed and how they are circulated among processors so as to maintain an even load on all processors.

The optimal partition of a graph according to various criteria is the subject of active research.[33] The cost of identifying an optimal partition is usually considered to be extremely high (NP-complete).[34] Since the search for an optimal partition could easily dwarf the cost of the exchange energy computation, we only consider here a heuristic approach that leads to a reasonable, if not optimal, distribution of the computational load.

The systolic algorithm described in ref 32 involves distributing orbitals among processors, computing exchange integrals between orbitals located on the same processor, and then rotating orbitals in a merry-go-round fashion, until all exchange integrals have been computed. The amount of work involved in this computation using p processors can be represented in terms of a $p \times p$ task matrix $\mathbf{T}$ whose elements t_{ij} represent the number of exchange integrals computed on processor i at rotation step j.

During one rotation step, an ideal distribution of orbitals would result in all diagonal elements of the matrix $\mathbf{T}$ being equal, i.e., all processors at that rotation step having an equal load. In order to maintain good load balancing, it is also necessary to maintain that property after orbitals are rotated among processors. This implies that the ideal task matrix should have the structure of a Toeplitz matrix,[35] i.e., have constant values along all its diagonals.

In an arbitrary system, it is unlikely that this goal can be achieved. The heuristic approach we use is based on the following argument. Orbitals can be classified according to the number of orbitals with which they overlap. This corresponds to labeling each node of the task graph with its degree. We then assign nodes to processors in a round-robin fashion in order of decreasing degree. The rationale behind this approach is that orbitals having a high degree give the largest contributions to the elements of the task matrix. The round-robin distribution based on decreasing degree is found to yield an even load distribution.

The implementation of this heuristic approach involves a permutation of the columns of the orthogonal matrix obtained from the simultaneous diagonalization procedure. This permutation only involves an $n \times n$ distributed matrix and therefore does not significantly add to the cost of the bisection algorithm. This parallel algorithm was implemented in the Qbox code.[36,37]

6. APPLICATIONS

In this section, we present applications of the recursive subspace bisection method to the computation of the electronic structure of a sample of liquid water including a chloride ion

$((H_2O)_{63}Cl^-)$ as well as the formation energy of a vacancy in bulk silicon using a 512-atom sample. We then discuss the application of the method to the computation of HOMO–LUMO gaps in water. Finally, we demonstrate that the error caused by this approach on ionic forces is small and can be controlled. We use the PBE0 hybrid exchange-correlation functional[12] and norm-conserving pseudopotentials[38,39] in all calculations.

A sample of $((H_2O)_{63}Cl^-)$ was extracted from a DFT molecular dynamics simulation performed using the PBE exchange-correlation functional[40] at a temperature of 400 K. Two levels of recursive bisection were used in each of the *x*, *y*, and *z* directions, leading to a total of six Walsh projectors. Table 1 shows the computational cost of a single Born–Oppenheimer MD step involving five self-consistent cycle iterations using various values of the truncation threshold. The speedup obtained is given as a function of the truncation threshold. The data in Table 1 show that the scalability of the algorithm is preserved when the RSB procedure is used.

Table 1. Time per MD Step for $(H_2O)_{63}Cl^-$ Using PBE0 on 1024 and 2048 Cores of an IBM BlueGene/P Computer

	1024 cores		2048 cores	
ε	time (s)	speedup	time (s)	speedup
0.000	672	1	308	1
0.002	311	2.2	161	1.9
0.005	234	2.9	126	2.4
0.010	191	3.5	105	2.9

Table 2 shows the computational cost of a Born–Oppenheimer MD step for a system of 256 water molecules.

Table 2. Time per MD Step for $(H_2O)_{256}$ Using PBE0 on 1536 Cores of a Cray XE6 Computer

ε	time (s)	speedup
0.0000	14000	1
0.0010	1179	11
0.0025	643	21
0.0050	425	33
0.0100	303	46
0.0250	162	86
0.0500	73	192

Three levels of recursive bisection were used in each direction, for a total of nine Walsh projectors. A comparison with Table 1 shows that a larger speedup is obtained as the size of the system increases.

Figure 1 compares the accuracy and cost of the computation of the total energy of $(H_2O)_{63}Cl^-$. The PBE0 ground state energy was calculated using increasing values of ε. Figure 1 shows that the error in the total energy of the entire system decreases smoothly to zero as the value of ε is reduced. For a value of $\varepsilon = 0.01$, the total energy error is approximately 0.01 au (5×10^{-5} au/atom). The corresponding computational cost is reduced by a factor of 4 compared to the exact calculation with $\varepsilon = 0$. Increasing the threshold value to $\varepsilon = 0.05$ leads to an error of 5×10^{-4} au/atom, and a speedup of about 10 compared to the exact calculation. Conversely, choosing a smaller threshold $\varepsilon = 0.002$ yields a total energy error of 0.0018 au (9.8×10^{-6} au/atom) for a speedup of about 2.5. These results show that recursive subspace bisection can be used with varying thresholds to control the error affecting the Hartree–Fock exchange energy.

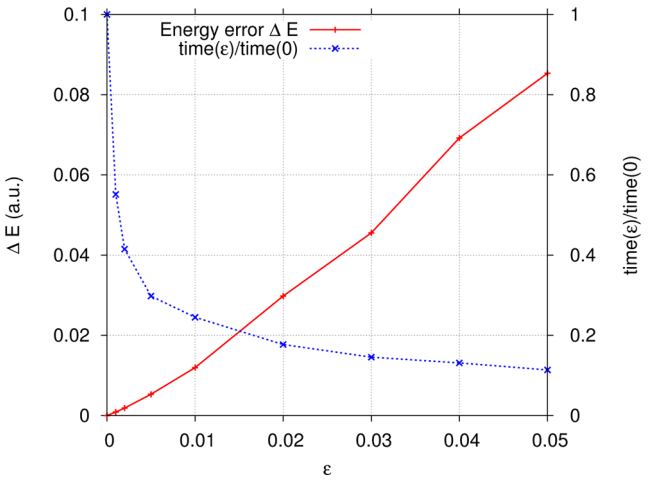

Figure 1. Error in the total energy (red solid line) and ratio of computing time (blue dotted line) obtained with various truncation thresholds of the recursive bisection method for the computation of the PBE0 energy of a $(H_2O)_{63}Cl^-$ sample.

The degree to which orbitals can be localized depends on the physical properties of the system under study. It is expected, on the basis of the arguments of Kohn,[41,42] that orbitals cannot be localized efficiently in systems having a small HOMO–LUMO band gap. In order to illustrate that effect, we have computed the vacancy formation energy in a silicon crystal using a 512-atom cell. The geometry of the vacancy was optimized using the PBE functional. The vacancy formation energy was then evaluated using the ground state energy of the bulk 512-atom cell and the 511-atom cell including the vacancy, computed self-consistently using the PBE0 hybrid functional and recursive subspace bisection. The calculations were repeated using various values of the threshold parameter. Table 3 shows the computed value of the vacancy formation energy as a function of the threshold parameter ε together with the corresponding speedup achieved through the bisection procedure. Even though the band gap of silicon is much smaller than that of the aqueous solution discussed above, the data in Table 3 show that a substantial speedup can still be achieved with a moderate error. A choice of $\varepsilon = 0.02$ yields a 5% error of 0.21 eV for a speedup of 4.95. This error may be acceptable for high-temperature MD simulations. If a higher accuracy is required, the threshold parameter must be reduced, resulting in a smaller speedup.

Table 3. Vacancy Formation Energy in Silicon Computed with the PBE0 Exchange-Correlation Functional and Various Values of the Threshold Parameter

ε	E_{vac} (eV)	speedup
0.000	4.429	1.00
0.005	4.434	1.76
0.010	4.612	3.77
0.020	4.636	4.95

6.1. HOMO–LUMO Gaps. The calculation of band gaps requires an additional constraint during the recursive bisection procedure to ensure that the orthogonal transformation obtained from the approximate simultaneous diagonalization does not mix the subspaces of occupied and empty orbitals.

dx.doi.org/10.1021/ct3007088 | J. Chem. Theory Comput. XXXX, XXX, XXX–XXX

This is done by setting to zero the matrix elements of the Walsh projectors that couple occupied and empty orbitals. As a result, the matrices used in the simultaneous diagonalization procedure have a block diagonal structure. This allows for the use of recursive bisection to accelerate the computation of band gaps when using hybrid density functionals. Table 4 shows the computed HOMO−LUMO gap in $(H_2O)_{63}Cl^-$ using the PBE0 hybrid functional and various values of the truncation threshold. The value of the gap is rather insensitive to the value of the threshold, with a 1.4% error (0.1 eV) for a threshold value of $\varepsilon = 0.05$.

Table 4. HOMO−LUMO Gap of a Snapshot of $(H_2O)_{63}Cl^-$ Computed with the PBE0 Exchange-Correlation Functional and Various Values of the Threshold Parameter

ε	E_g (eV)
0.0	7.03
0.01	7.01
0.02	6.99
0.05	6.92

6.2. Molecular Dynamics Simulations. The accuracy of first-principles molecular dynamics (MD) simulations and of the statistical averages derived from them depends critically on the accuracy of computed ionic forces. Time-reversibility of the MD integration scheme is important in order to ensure accuracy of the results.[43] It is therefore important to assess the impact of the recursive subspace bisection method on computed ionic forces. We have evaluated this effect using snapshots from a first-principles molecular dynamics simulation of a 64-molecule sample of water performed with the PBE density functional. Ionic forces were computed using the PBE0 ground state orbitals and various thresholds of recursive subspace bisection. Errors in the ionic force components were collected for each threshold value. Figure 2 (upper panels) shows histograms of the errors in ionic force components caused by the use of recursive bisection with thresholds $\varepsilon = 0.005$ (a) and $\varepsilon = 0.01$ (b). These errors are compared with the errors caused by changing the plane wave energy cutoff from 85 to 100 Ry (c, lower panel). The error caused by recursive subspace bisection is considerably smaller than that caused by the change in basis set. This change in basis set was found to cause negligible changes in statistical properties of water in first-principles molecular dynamics simulations. We have tested the constant of the motion in several Born−Oppenheimer PBE0 simulations of liquid water. It was found that the use of recursive subspace bisection causes small fluctuations in the constant of the motion (~1% of the ionic kinetic energy) but no appreciable drift.

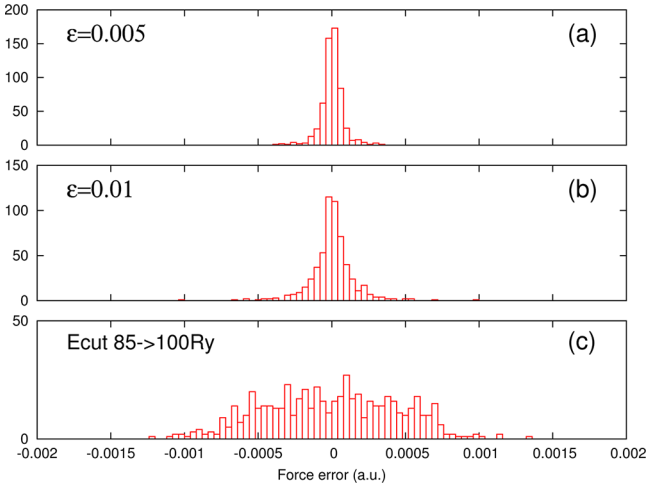

Figure 2. Histograms of errors in ionic forces caused by the use of the recursive bisection method for a $(H_2O)_{64}$ sample (a,b) and by a change in the plane wave energy cutoff from 85 to 100 Ry (c).

The results presented above demonstrate how the threshold parameter can be used to control the accuracy of calculated energies and ionic forces. It should be noted that the threshold parameter can be changed during the course of a calculation, in particular between SCF iterations. This opens the possibility of using a dynamical scheme in which a coarse threshold is progressively reduced during the calculation, leading to substantial savings in computing time even if the fully accurate (zero-threshold) result is desired at the end.

7. CONCLUSIONS

We have shown that the recursive subspace bisection method introduced in ref 16 can be used to accelerate the calculation of the Hartree−Fock exchange energy in plane-wave, pseudopotential electronic structure calculations, while preserving a controlled accuracy. A parallel implementation and a load balancing algorithm are discussed, and a substantial speedup is demonstrated in simulations of a 64-molecule water sample using the PBE0 hybrid density functional. A larger acceleration is obtained for larger systems. A threshold parameter is used to control the error caused by truncation of the orbitals in subdomains of the simulation cell. Reducing the threshold parameter gradually to zero reduces the truncation error and leads back to the original cost of the Hartree−Fock exchange calculation. Calculations of HOMO−LUMO gaps can be accelerated using the same approach. The error in ionic forces is also shown to be controlled by the threshold parameter. The method presented greatly extends the range of feasible first-principles simulations using hybrid density functionals.

AUTHOR INFORMATION

Corresponding Author

*E-mail: fgygi@ucdavis.edu.

Notes

The authors declare no competing financial interest.

ACKNOWLEDGMENTS

We would like to thank G. Galli for numerous discussions. This work was supported by the National Science Foundation through grant OCI 0749217. Allocation of computing resources by NSF XSEDE through the award TG-ASC090004 is gratefully acknowledged. An award of computer time was provided by the DOE Innovative and Novel Computational Impact on Theory and Experiment (INCITE) program. This research used resources of the Argonne Leadership Computing Facility at Argonne National Laboratory, which is supported by the Office of Science of the U.S. Department of Energy under contract DE-AC02-06CH11357.

REFERENCES

(1) Hohenberg, P.; Kohn, W. *Phys. Rev.* **1964**, *136*, B864−B871.

(2) Dreizler, R. M.; Gross, E. K. U. *Density Functional Theory: An Approach to the Quantum Many-Body Problem*; Springer: New York, 1990.
(3) Kohn, W.; Sham, L. J. *Phys. Rev.* **1965**, *140*, A1133−A1138.
(4) Tao, J.; Perdew, J. P.; Staroverov, V. N.; Scuseria, G. E. *Phys. Rev. Lett.* **2003**, *91*, 146401.
(5) Becke, A. D. *Phys. Rev.* **1988**, *A38*, 3098−3100.
(6) Becke, A. D. *J. Chem. Phys.* **1993**, *98*, 5648.
(7) Lee, C.; Yang, W.; Parr, R. G. *Phys. Rev.* **1988**, *B37*, 785.
(8) Curtiss, L. A.; Raghavachari, K.; Trucks, G. W.; Pople, J. A. *J. Chem. Phys.* **1991**, *94*, 7221−7230.
(9) Xu, X.; Goddard, W. A. *Proc. Natl. Acad. Sci.* **2004**, *101*, 2673−2677.
(10) Chai, J.-D.; Head-Gordon, M. *J. Chem. Phys.* **2008**, *128*, 084106.
(11) Perdew, J. P.; Ernzerhof, M.; Burke, K. *J. Chem. Phys.* **1996**, *105*, 9982.
(12) Adamo, C.; Barone, V. *J. Chem. Phys.* **1999**, *110*, 6158.
(13) Heyd, J.; Scuseria, G. E.; Ernzerhof, M. *J. Chem. Phys.* **2003**, *118*, 8207.
(14) Henderson, T. M.; Izmaylov, A. F.; Scalmani, G.; Scuseria, G. E. *J. Chem. Phys.* **2009**, *131*, 044108.
(15) Zhang, C.; Donadio, D.; Gygi, F.; Galli, G. *J. Chem. Theory Comput.* **2011**, *7*, 1443.
(16) Gygi, F. *Phys. Rev. Lett.* **2009**, *102*, 166406.
(17) Whitten, J. L. *J. Chem. Phys.* **1973**, *58*, 4496.
(18) Häser, M.; Ahlrichs, R. *J. Comput. Chem.* **2004**, *10*, 104−111.
(19) Strain, M. C.; Scuseria, G. E.; Frisch, M. J. *Science* **1996**, *271*, 51−53.
(20) Challacombe, M.; Schwegler, E. *J. Chem. Phys.* **1997**, *106*, 5526.
(21) Burant, J.; Scuseria, G.; Frisch, M. *J. Chem. Phys.* **1996**, *105*, 8969.
(22) Schwegler, E.; Challacombe, M.; Head-Gordon, M. *J. Chem. Phys.* **1997**, *106*, 9708.
(23) Ochsenfeld, C.; White, C. A.; Head-Gordon, M. *J. Chem. Phys.* **1998**, *109*, 1663−1669.
(24) Yanai, T.; Fann, G. I.; Gan, Z.; Harrison, R. J.; Beylkin, G. *J. Chem. Phys.* **2004**, *121*, 6680−6688.
(25) Harrison, R. J.; Fann, G. I.; Yanai, T.; Gan, Z.; Beylkin, G. *J. Chem. Phys.* **2004**, *121*, 11587−11598.
(26) Giannozzi, P.; Baroni, S.; Bonini, N.; Calandra, M.; Car, R.; Cavazzoni, C.; Ceresoli, D.; Chiarotti, G. L.; Cococcioni, M.; Dabo, I.; Dal Corso, A.; de Gironcoli, S.; Fabris, S.; Fratesi, G.; Gebauer, R.; Gerstmann, U.; Gougoussis, C.; Kokalj, A.; Lazzeri, M.; Martin-Samos, L.; Marzari, N.; Mauri, F.; Mazzarello, R.; Paolini, S.; Pasquarello, A.; Paulatto, L.; Sbraccia, C.; Scandolo, S.; Sclauzero, G.; Seitsonen, A. P.; Smogunov, A.; Umari, P.; Wentzcovitch, R. M. *J. Phys. C: Condens. Matter* **2009**, *21*, 395502 (19pp).
(27) Gonze, X.; Beuken, J.-M.; Caracas, R.; Detraux, F.; Fuchs, M.; Rignanese, G.-M.; Sindic, L.; Verstraete, M.; Zerah, G.; Jollet, F.; Torrent, M.; Roy, A.; Mikami, M.; Ghosez, P.; Raty, J.-Y.; Allan, D. *Comput. Mater. Sci.* **2002**, *25*, 478−492.
(28) Paier, J.; Hirschl, R.; Marsman, M.; Kresse, G. *J. Chem. Phys.* **2005**, *122*, 234102.
(29) Massidda, S.; Posternak, M.; Baldereschi, A. *Phys. Rev.* **1993**, *B48*, 5058.
(30) Wu, X.; Selloni, A.; Car, R. *Phys. Rev. B* **2009**, *79*, 085102.
(31) Boys, S. F. *Rev. Mod. Phys.* **1960**, *32*, 296.
(32) Duchemin, I.; Gygi, F. *Comput. Phys. Commun.* **2010**, *181*, 855−860.
(33) Hendrickson, B.; Kolda, T. *Parallel Comput.* **2000**, *26*, 1519−1534.
(34) Garey, M.; Johnson, D.; Stockmeyer, L. *Theor. Comput. Sci.* **1976**, *1*, 237−267.
(35) Horn, R.; Johnson, C. *Matrix Analysis*; Cambridge University Press: Cambridge, U. K., 1990.
(36) Gygi, F. *IBM J. Res. Dev.* **2008**, *52*, 137.
(37) http://eslab.ucdavis.edu/software/qbox (accessed Nov 9, 2012).
(38) Hamann, D. R.; Schlüter, M.; Chiang, C. *Phys. Rev. Lett.* **1979**, *43*, 1494−1497.
(39) Vanderbilt, D. *Phys. Rev. B* **1985**, *32*, 8412−8415.
(40) Perdew, J. P.; Burke, K.; Ernzerhof, M. *Phys. Rev. Lett.* **1996**, *77*, 3865−3868.
(41) Kohn, W. *Phys. Rev. Lett.* **1996**, *76*, 3168−3171.
(42) Prodan, E.; Kohn, W. *Proc. Natl. Acad. Sci. U. S. A.* **2005**, *102*, 11635−11638.
(43) Niklasson, A.; Tymczak, C.; Challacombe, M. *Phys. Rev. Lett.* **2006**, *97*, 123001.